

Aerosol Science and Technology

ISSN: 0278-6826 (Print) 1521-7388 (Online) Journal homepage: https://www.tandfonline.com/loi/uast20

Ultrafine Particle Generation at High Liquid Flow Rates with Commercial Two-Fluid Nozzles

Cynthia LeCompte Salisbury , Gurdal Tuncel & John M. Ondov

To cite this article: Cynthia LeCompte Salisbury , Gurdal Tuncel & John M. Ondov (1991) Ultrafine Particle Generation at High Liquid Flow Rates with Commercial Two-Fluid Nozzles, Aerosol Science and Technology, 15:3, 156-169, DOI: 10.1080/02786829108959522

To link to this article: https://doi.org/10.1080/02786829108959522

Published online: 08 Jun 2007.

Submit your article to this journal

Article views: 422

View related articles

Citing articles: 4 View citing articles

Full Terms & Conditions of access and use can be found at
https://www.tandfonline.com/action/journalInformation?journalCode=uast20

Ultrafine Particle Generation at High Liquid Flow Rates with Commercial Two-Fluid Nozzles

Cynthia LeCompte Salisbury,* Gurdal Tuncel,† and John M. Ondov
Department of Chemistry and Biochemistry, University of Maryland, College Park, MD 20742

Residue particles with volume median diameters ranging from 23 to 68 nm were made by dispersing KNO_3 or $MnCL_2 \cdot 4H_2O$ solutions with commercially available pneumatic nozzles at liquid flow rates of 0.07 and 0.021 cm^3/s and atomizing air pressures (gauge) ranging from 276 to 3447 kPag. Droplets with median diameters of 1.5 ± 0.3 μm were made at the 0.07 cm^3/s liquid flow rate, which represents a nearly 10-fold increase in liquid flow rate achieved with Collison atomizers used to generate droplets of similar sizes under conditions specified by their manufacturers.

INTRODUCTION

Particles with diameters < 100 nm can be made in the laboratory with simple Collison nebulizers by dispersing dilute solutions containing a volatile solvent. Collison nebulizers employ one or more two-fluid nozzles in which liquid from a reservoir is aspirated by the Bernouli pressure drop created in the region of an orifice by a stream of rapidly moving air. The energy in compressed gas disperses the jet of liquid into droplets. The residue particle size varies inversely with the cube root of the mass concentration of the solute, and can be calculated if the residue particle density is known (Mercer, 1973). Two-fluid nozzles are typically operated at air pressures ranging from 100 to 700 kPag and produce droplets with median diameters ranging from about 10 to 100 μm. In nebulizers, small droplet median diameters, e.g., from 1.65 to 2 μm (BGI, 1990), are achieved by impaction of large droplets. Median residue particle diameters substantially < 100 nm are achievable with these systems, however, as large droplets comprise as many as 98% of the particles produced (Mercer, 1973), liquid droplet generation rates are quite small, typically < 0.5 mL/min per atomizer when operated under conditions specified by the manufacturer.

In two-fluid nozzles, droplet size depends strongly on the ratio of the mass flow rates of air and liquid, and dynamic force ($\rho \cdot V_{rel}^2$, where V_{rel} is the relative velocity between the gas and the liquid, and ρ is the gas density), and thus tends to decrease with increasing gas pressure (Kim and Marshal, 1971). However, in Collison nebulizers, liquid flow rate also increases with increasing atomizing pressure and very little decrease in droplet size is achieved by increasing air pressure. Empirical equations for two-fluid nozzles show that mean droplet size decreases (a) as the ratio of the mass flow rates of air to that of liquid increases, (b) with increasing dynamic force, and (c) with decreasing surface tension (σ); and therefore, droplet size decreases with increasing Weber number ($D_l \cdot V_{rel}^2 \cdot \rho / \sigma$; where D_l is the liquid orifice diameter (see Kim and Marshall, 1971; Mercer, 1973. Herein, V_{rel} is calculated at the nozzle throat). Glukov's equation (Mercer, 1973) also shows a first-order dependence on the diameter of the liquid orifice and suggests that droplets

*Present address: Booz-Allen and Hamilton, 4330 Eastwest Highway, Bethesda, MD 20814.
†Present address: Environmental Engineering Department, Middle East Technical University, Ankara 06531, Turkey.

0278-6826/91/$3.50
Aerosol Science and Technology 15:156-169 (1991)
© 1991 Elsevier Science Publishing Co., Inc.

with diameters comparable to those obtained from pneumatic atomizers might be obtained by judicious choice of D_l, atomizing pressure, liquid flow rate, and liquid surface tension, but at higher liquid outputs.

Kim and Marshall (1971) have shown that increasing pressure (and, hence, dynamic force) is accompanied by a decrease in the atomizing efficiency (i.e., the fraction of the energy of the gas which is used in forming droplets) which leads to a lower limit in the droplet size achievable. They made droplet size correlations for various convergent-type, concentric-orifice, air-atomizing nozzles for gas/liquid mass flow rate ratios ranging from 0.06 to 40 and Webber numbers (N_{We}) ranging from 180 to 30,000, and reported a minimum droplet mass median diameter (MMAD) of 6 μm with a nozzle made by the Spraying Systems Company (SSC Wheaton).

The extrapolation of droplet size outside the range of experimental air pressure and liquid flow rate is complicated because changes in the nature of the breakup process occur as fluid and geometry parameters change. Kim and Marshall (1971), for example, have observed high pressure cavitation, in which atomizing gas invades the liquid orifice causing the liquid to issue as a cylindrical film rather than a solid jet as is the case at lower pressures. Thus, extrapolations must be verified experimentally.

Our interest was in generating large quantities of ultrafine (e.g., diameter < 50 nm) tracer particles for use in *in situ* fly ash tagging studies to be conducted at a coal-fired power plant (Ondov and Kelly, 1990). Liquid dispersal rates > 50 mL/min were needed to achieve a minimum aerosol output of 10 mg/h, using 3-ppm solutions of separated rate-earth isotopic tracer materials, a rate not conveniently achieved with a practical number of Collison nebulizers operated at conditions specified by the manufacturer. Herein, we describe the generation of residue particles with MMADs between 20 and 70 nm with liquid output rates ≤ 4.4 mL/min per nozzle using industrial two-fluid air atomizing nozzles operated at gas/liquid mass flow rate ratios and N_{We} ranging from 5 to 250 and 7100 to 225,000, respectively. The nozzles tested are suitable for use *in situ* in the harsh power plant flue gas environment and could provide the minimum requisite liquid output with a practical array of 12 nozzles.

EXPERIMENTAL MEASUREMENTS

Three commercially available air atomizing nozzles were selected for testing: a Sonicore nozzle made by Sonic Energy Systems (Willmington) and two 1/4J nozzles made by the SSC. Each of these mixes air and fluid inside rather than outside the nozzle. The Sonicore nozzle is a convergent, divergent type in which liquid is introduced at nearly right angles to the flow (Figure 1*a*). The SSC nozzles are convergent concentric ori-

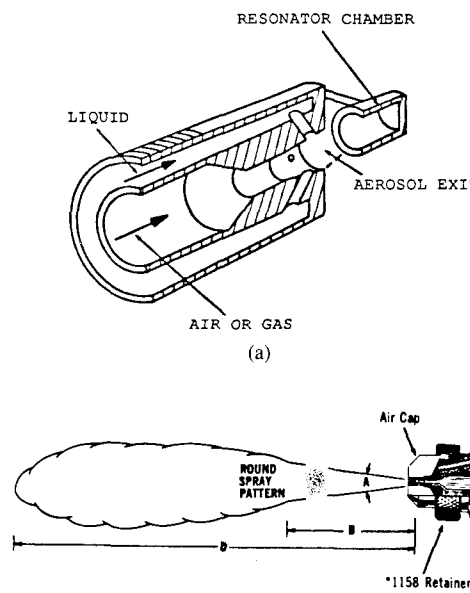

FIGURE 1. Schematic drawings of (*a*) Sonicore and (*b*) SSC nozzles.

TABLE 1. Characteristics of Air Atomizing Nozzles Chosen for Testing

Nozzle	Manufacturer	Type	Liquid orifice diameter (μm)	Air orifice dimension (μm)	Spray pattern
Sonicore	Sonic Energy Systems	Radial liquid injection	899	1000[a]	Round (without cap)
SSC-1[b]	Spraying Systems Co.	Concentric orifice	711 (2850 liq. cap)[d]	432[c]/1194[a] (67147 air cap)[e]	Round
SSC-2[b]	Spraying Systems Co.	Concentric orifice	508 (2050 liquid cap)[d]	432[b]/1194[a] (67147 air cap)[e]	Round

[a]Orifice diameter.
[b]Model number is 1/4J plus the liquid and air cap codes.
[c]Annulus width.
[d]In liquid cap codes the first and second two digits are the liquid orifice, i.d. and o.d., in thousandths of an inch.
[e]The first two digits of the air cap code are the inlet diameter of the air orifice; the third digit indicates the spay pattern (1 = round spray) and the last two digits are the diameter of the air orifice at the outlet for round spray nozzles.

fice nozzles in which air is introduced through an annulus around the liquid orifice (Figure 1*b*). Air and liquid orifices are readily selected for SSC nozzles by installing interchangeable air and liquid caps on the nozzle body. The two SSC nozzle configurations used the same air cap, but the second configuration (SSC-2) was fitted with a smaller liquid orifice to investigate the effect of nozzle diameter on droplet size. The characteristics of these nozzles are listed in Table 1.

The effects of atomizing air pressure on residue particle size were investigated at pressures ranging from 276 to 6893 kPag and liquid flow rates of 0.074 and 0.021 cm^3/s as indicated in Table 2. Herein, gas pressures refer to the pressure of the reservoir, upstream of the nozzle throat, measured relative to ambient pressure, i.e. gauge pressure. Initial tests were performed with aqueous solutions containing 3 ppm (mass/volume) KNO_3; however, water was abandoned in favor of methanol ("Analyzed Reagent," J. T. Baker Co., Phillipsburg, NJ, 0.1–0.4 ppm residue after evaporation) because aerosol made from aqueous solutions contained droplets larger than 0.5 μm, whereas aerosol made from methanol solutions did not (Figure 2). In addition to its greater volatility, the surface tension and viscosity of methanol are three- and twofold lower, respectively, which favor the production of smaller droplets. As indicated in Table 2, additional tests were made with solutions made from $MnCl_2 \cdot 4H_2O$ in absolute methanol to permit detection by instrumental neutron activation analysis (INAA).

All of the tests were conducted in 8.5-m long, 0.9×0.9-m plexiglass test chamber

TABLE 2. Operating Parameters in Air Atomizing Nozzle Tests

Nozzle	Solution	Liquid flow rate (cm^3/s)	Atomizing air pressure[a] (kPag)
SSC-1	3 ppm KNO_3 in MeOH	0.074	276–1585
	11 ppm $MnCl_2 \cdot 4H_2O$ in MeOH	0.074	1585–3447
SSC-2	11 ppm $MnCl_2 \cdot 4H_2O$ in MeOH	0.074	1585
Sonicore	3 ppm KNO_3 in MeOH	0.021	689, 2757
		0.071	689–2757
	11 ppm $MnCl_2 \cdot 4H_2O$ in MeOH	0.074	2757, 6893

[a]Gauge pressure.

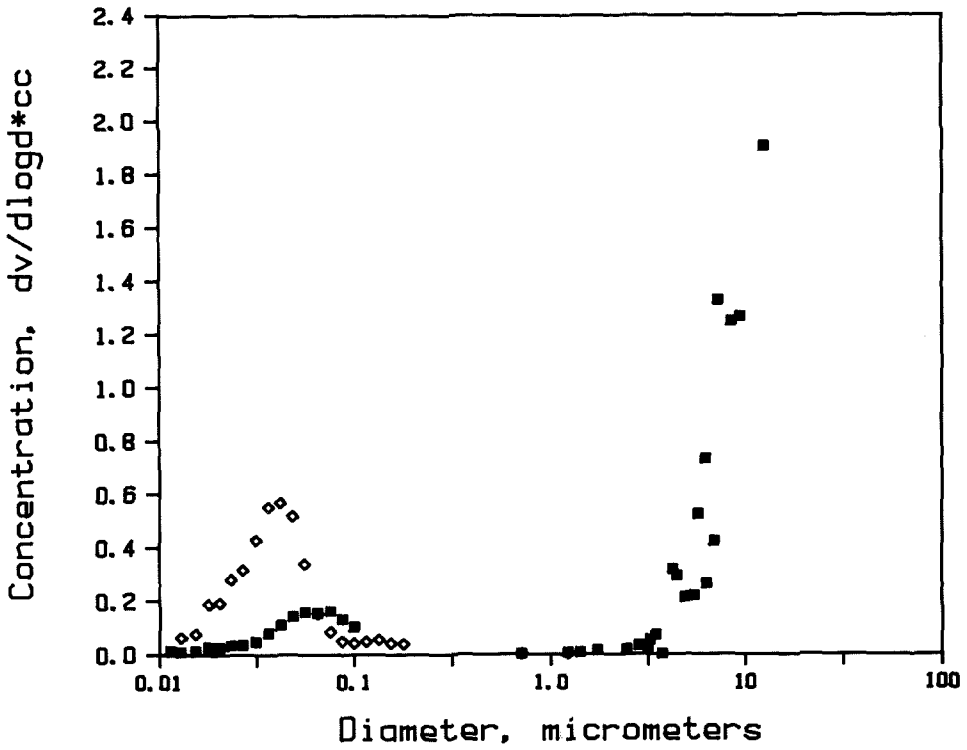

FIGURE 2. Number concentration vs. particle size distributions show that aerosol made from aqueous solutions contained droplets larger than 0.5 μm in diameter (■). Aerosol made from absolute methanol solutions (◇) did not. Particles < 0.5 μm in diameter were measured with the DMA-CNC; particles ≥ 0.5 μm were measured with the CSAS-100.

with HEPA-filtered air flowing at a velocity of 0.5 m/s. The test nozzles were mounted along the central axis of the chamber near the inlet. Residue particle size measurements were made at a distance of 6 m downstream from the nozzle, shortly after the aerosol plume spread to the walls of the chamber. At this distance from the nozzle, mixing of the nozzle plume and chamber dilution air was complete (Figure 3). Losses to the wall of the chamber were evaluated previously for Nd aerosol by attaching filter papers on the inside wall. Instrumental neutron activation analyses of the filter papers showed that wall losses for the Nd aerosol were negligible.

Number distributions of residue particles with nominal diameters between 10 nm and 1 μm were measured with a Thermo Systems, Inc. (St. Paul, MN) model 3071 differential mobility analyzer (DMA) with a model 3020 continuous condensation nucleus counter (CNC) as the detector. The DMA-CNC were located outside the chamber and aerosol was extracted from the center of the chamber through a 4.4-mm-i.d., 65-cm stainless steel probe with a 90° bend 3 cm from the inlet end. The probe was connected directly to the DMA inlet impactor. Some initial measurements of particles with diameters between 0.5 and 10 μm (Figure 2) were made with a Particle Measurements Systems (Boulder, CO) CSAS-100, high-volume forward-scattering laser spec-

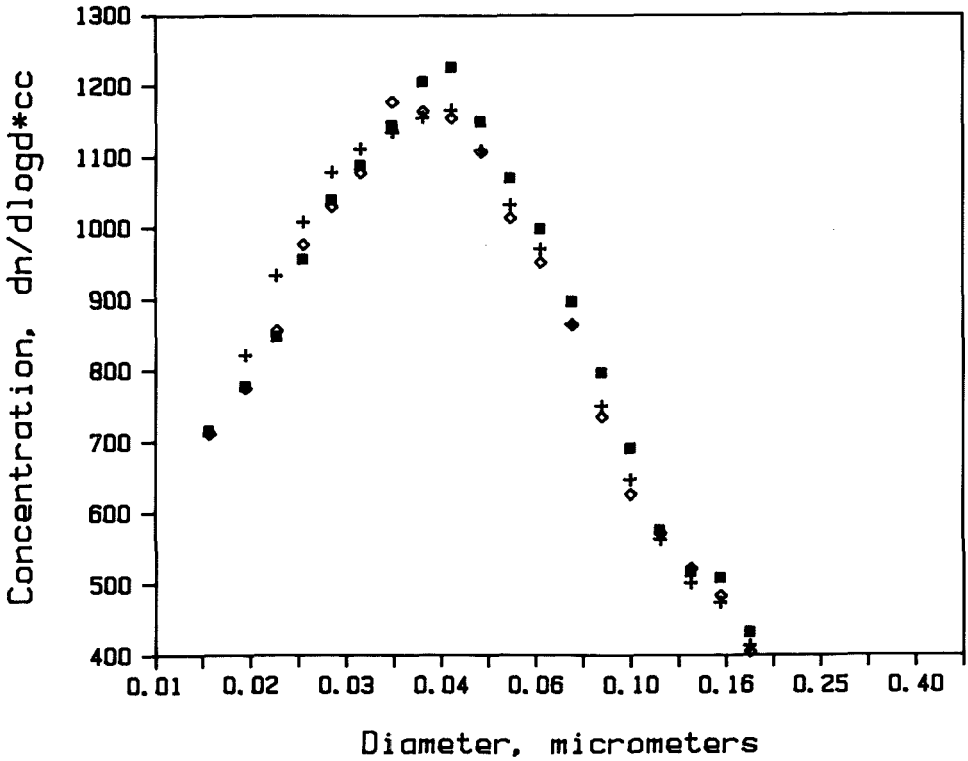

FIGURE 3. Number vs. size distributions of particles produced with nozzle SSC-1 at the center (■), near the wall (◇), and midway between the center and the wall (+) of the test chamber at a distance of 6.1 m from the nozzle.

trometer mounted inside the test chamber with its inlet facing into the gas stream towards the nozzle. However, as shown in Figure 2, concentrations of particles in this size range were insignificant when methanol solutions were aspirated. The number concentrations of particles too small to size in the DMA were estimated as the difference between the CN count for the total aerosol and the sum of all particles measured with the DMA-CNC. This was done by alternately connecting the CNC or DMA to the 65-cm sampling probe. Corrections for diffusional losses in the DMA were made using the algorithm of Reineking and Porstendorfer (1986). Losses in the probe were corrected using a similar algorithm (Parker, 1968).

In some cases, the sizes of individual particles were also determined with scanning or transmission electron microscopy (SEM and TEM). Some additional measurements were made of particles made from Mn solutions with a five-stage micro-orifice impactor (MOI) with integral backup filter (Kuhlmey et al., 1981; Marple et al., 1981) mounted inside the test chamber. Aerosol was sampled isokinetically through a 10-cm long, 3-cm i.d. inlet. The D_{50}'s (i.e., the diameters of particles collected with 50% efficiency) for the MOI ranged from 42 to 1050 nm (Marple and Rubow, 1984). Manganese mass collected on impactor stages were determined by INAA using the National Bureau of Standards 20-MW research reactor in Gaithersburg, MD. Gamma-ray spectra were measured on intrinsic Ge or Ge(Li) detectors.

RESULTS AND DISCUSSION

Effect of Atomizing Air Pressure

Results of tests to determine the performance of the Sonicore and SSC-1 nozzles at pressures ranging, respectively, from 689 to 2757 and from 276 to 1585 kPag with solutions containing 3 ppm KNO_3 in methanol and a liquid flow rate of 0.074 cm^3/s are shown in Figures 4 and 5. As shown in

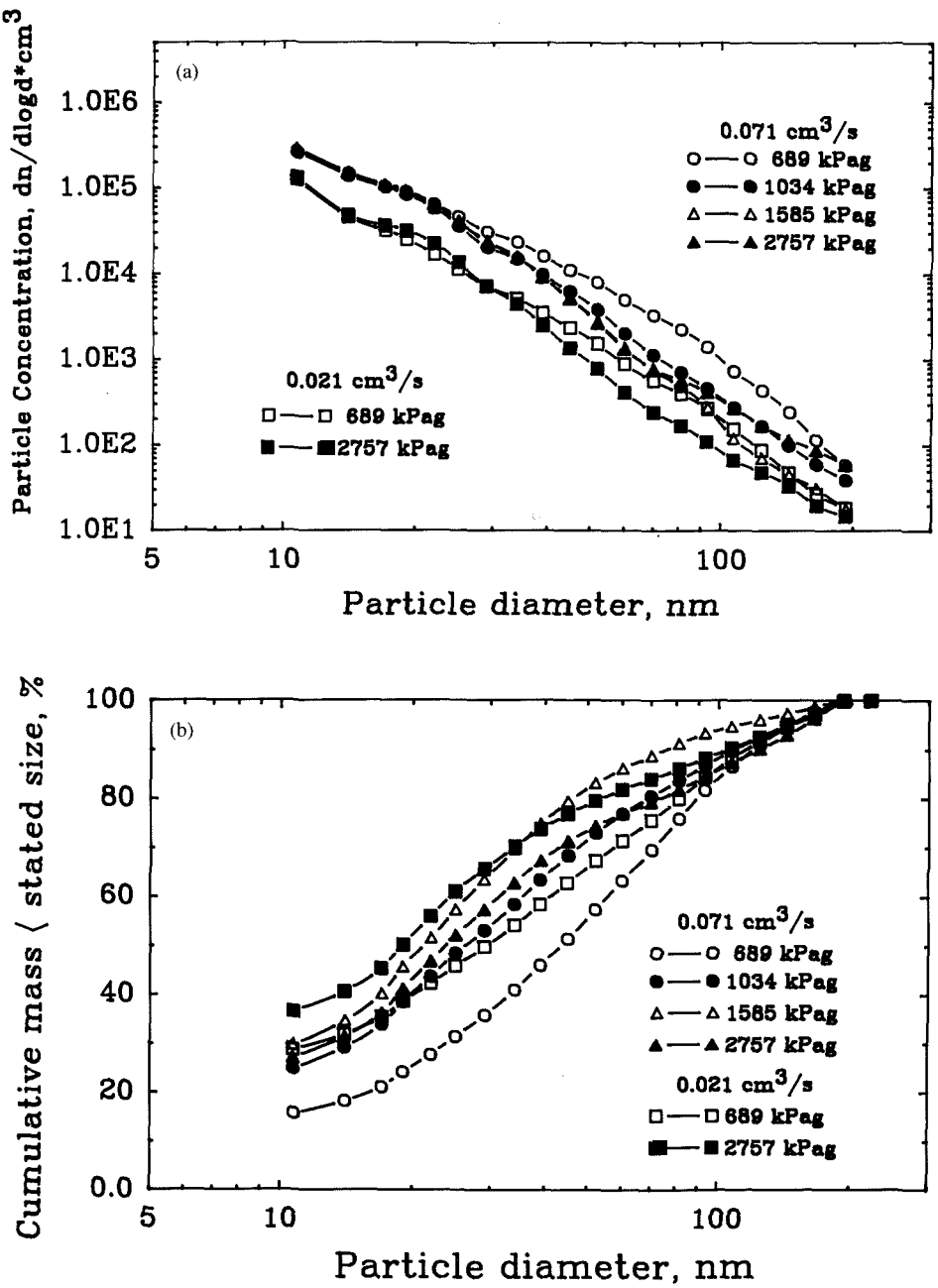

FIGURE 4. (*a*) Number and (*b*) cumulative volume vs. the diameter of KNO_3 residue particles made with the Sonicore nozzle.

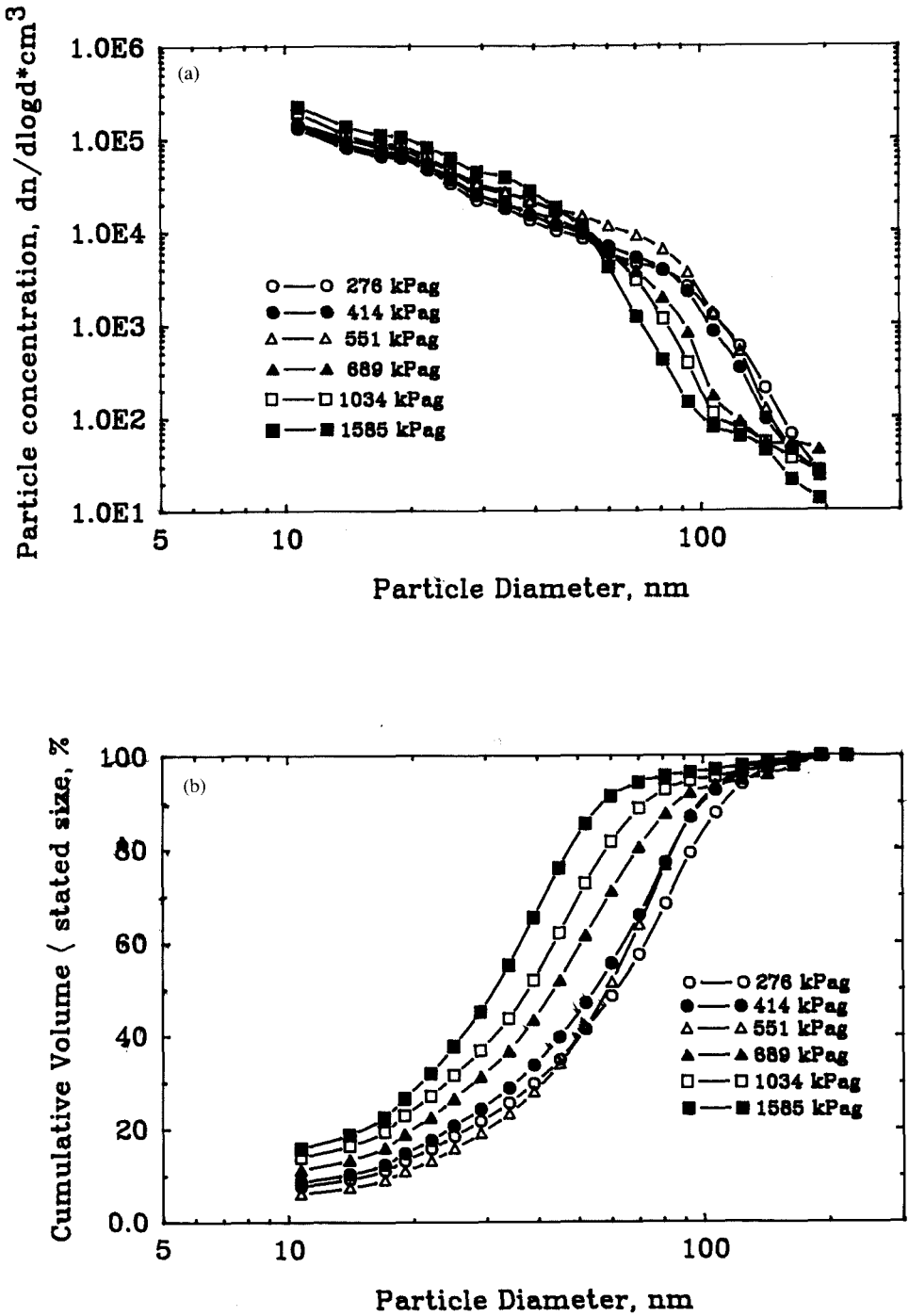

FIGURE 5. (*a*) Number and (*b*) cumulative volume vs. the diameter of KNO_3 residue particles made with nozzle SSC-1.

Figure 4*a*, the number distributions obtained with the Sonicore nozzle show a principal mode at about 18 nm, but another mode is evident by upturns in the distributions at a diameter < 12 nm. Distributions observed for nozzle SSC-1 (Figure 5*a*) also contained a mode at about 18 nm, but the mode below 12 nm was less prevalent than for the Sonicore data. In each case, the position of the 18-nm mode was little affected by increasing air pressure, but the fraction of particles < 25 nm increased at the expense of particles larger than this size. In essence, fewer larger droplets were made at higher pressures.

As shown by the cumulative volume curves in Figure 5*b*, increasing atomizing air pressure on the SSC-1 nozzle was accompanied by a progressive reduction in the volume median diameter ($VMAD_r$) of residue particles, except for the point at 551 kPag. Including this point, estimates of the $VMAD_r$'s achieved with this nozzle (e.g., 68, 60, 64, 48, 42, and 35 nm) vary nearly with the inverse of the atomizing air pressure raised to the power 0.40, i.e., somewhat less than the 0.45 exponent found by Glukov (Mercer, 1973) and Kim and Marshall (1971) for different nozzle configurations operated at smaller values of the dynamic force (Figure 6). Note that for a sonically operated nozzle, the gas velocity at the nozzle throat is a constant (Anderson, 1982) and the liquid velocity is negligible relative to the gas velocity. Thus, dynamic force is directly proportional to gas pressure and, for a given liquid, directly proportional to the Webber number, also. At pressures > 689 kPag, the $VMAD_r$'s achieved with the Sonicore nozzle were consistently

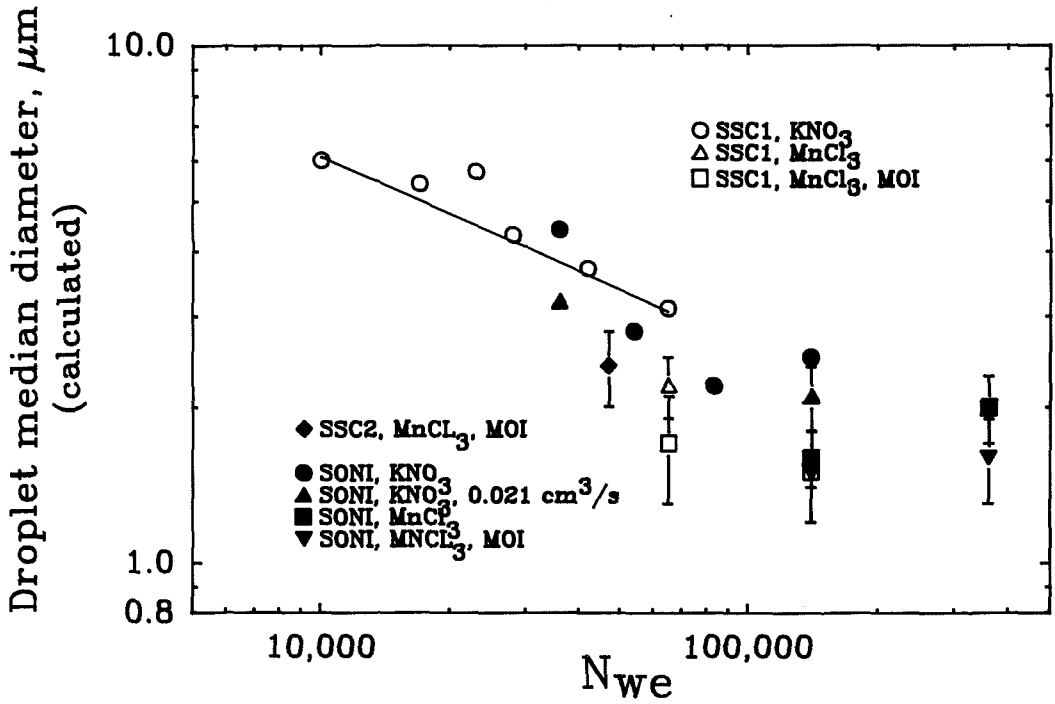

FIGURE 6. Estimates of the median aerodynamic diameters vs. Webber number for droplets made with the SSC and Sonicore nozzles listed in Table 3.

smaller than those achieved with nozzle SSC-1 at a similar liquid flow rate. As shown in Table 3, $VMAD_r$ decreased from 49.6 to 25.2 nm when atomizing pressure was increased from 689 to 1585 kPag. At 2757 kPag (liquid flow rate of 0.071 cm^3/s) a larger $VMAD_r$ (28.5 nm) was observed for the Sonicore nozzle. Smaller $VMAD_r$'s were obtained for the same atomizing pressure when the liquid flow rate was reduced from 0.071 to 0.021 cm^3/s.

In these data, the volume associated with particles smaller than the minimum DMA channel (i.e., 12 nm in tests with KNO_3 aerosol; 10 nm for $MnCL_2 \cdot 4H_2O$ aerosol) is uncertain because their size distribution is unknown and their concentrations are in error because the efficiency (ϵ) of the CNC drops off very rapidly below this size. In constructing the volume distributions, it was necessary to assume a volume mean diameter for these particles. To do this we fit the CNC efficiency data of Agarwal and Sem (1980) as reported by Bartz et al. (1985) and plotted the efficiency- and probe-loss-corrected particle volume function $(4/3 \cdot \pi \cdot (d/2)^3/\epsilon'$, where ϵ' is the product of the counting and transmission efficiencies for particles entering the CNC and sampling probe) against particle size. As shown by curve *b* in Figure 7, for particle diameters ranging from 3 to 12 nm, this function ranges between 0.064 and 0.19. The median value of this range, i.e., 0.125, corresponds to a particle diameter of 10.1 nm. Use of the latter gives a maximum error in the calculated particle volume of $\pm 50\%$ in the KNO_3 aerosol measurements made with nozzle

TABLE 3. Median Aerodynamic Diameters of Particles Made with Air Atomizing Nozzles

Nozzle	Solute	Instrument	Pressure[a] (kPag)	Median diameter residue[b] (nm)	Droplet[c] (μm)
SSC-1	KNO_3	DMA-CNC	276	68.0	6.0
			414	60.3	5.4
			551	64.4	5.7
			689	48.3	4.3
			1034	42.1	3.7
			1585	35.0	3.1
	$MnCl_2 \cdot 4H_2O$	DMA-CNC	1585	$43.6(1.7 \pm 0.3)^d$	2.2 ± 0.3
		MOI	1585	34 ± 5^e	1.7 ± 0.4
		DMA-CNC	3447	$42(1.6 \pm 0.2)^d$	2.1 ± 0.3
		MOI	3447	30 ± 3^e	1.5 ± 0.3
SSC-2	$MnCl_2 \cdot 4H_2O$	MOI	1585	48 ± 3^e	2.4 ± 0.4
Sonicore	KNO_3	DMA-CNC	689[f]	49.6	4.48
			1034[f]	31.9	2.8
			1585[f]	25.2	2.2
			2757[f]	28.5	2.5
			689[g]	36.4	3.2
			2757[g]	23.1	2.1
	$MnCl_2 \cdot 4H_2O$	DMA-CNC	2757	$33(1.85 \pm 0.15)^d$	1.6 ± 0.2
		MOI	2757	30 ± 2^e	1.5 ± 0.3
		DMA-CNC	6893	$40.4(1.84 \pm 0.20)^d$	2.0 ± 0.3
		MOI	6893	33 ± 3^e	1.6 ± 0.3

[a]Atomizing air pressure.
[b]Volume or mass median aerodynamic diameter of residue particles.
[c]Estimated droplet median diameter based on median size of residue particles.
[d]Geometric standard deviation determined from cumulative volume plots.
[e]Value estimated from MOI data as described in the text.
[f]Liquid flow rate was 0.071 cm^3/s.
[g]Liquid flow rate was 0.021 cm^3/s.

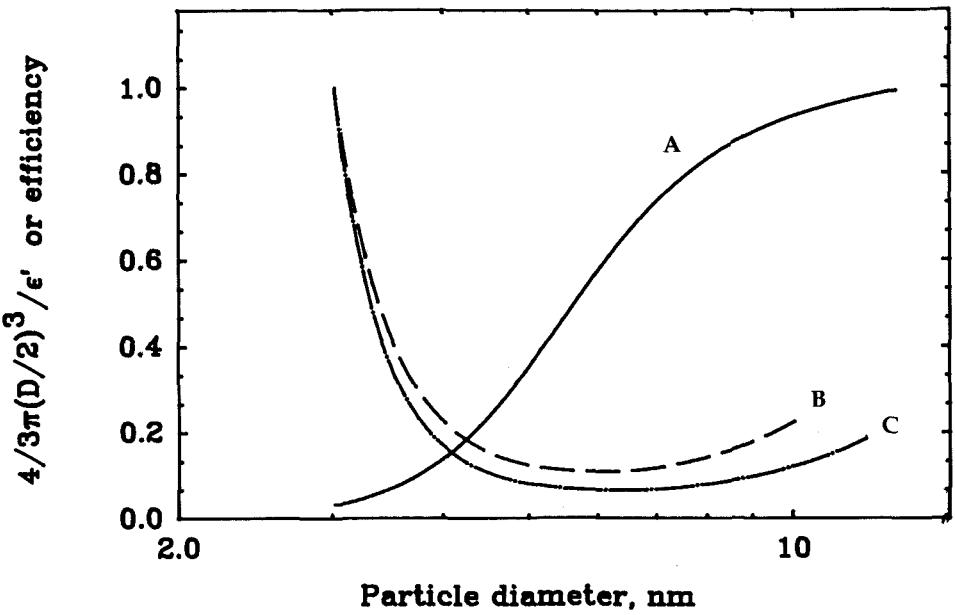

FIGURE 7. (*a*) The CNC efficiency and (*b* and *c*) relative efficiency-corrected particle volume curves vs. particle size.

SSC-1, however, the corresponding error in the fraction of aerosol volume contained in particles smaller than 12 nm is somewhat less, i.e., ±35%, and leads to only a ±3% error in the VMADs. For KNO_3 particles made with the Sonicore nozzle, this assumption leads to an uncertainty of about ±10% in the $VMAD_r$. Because of these uncertainties, additional tests were made using the MOI at the 0.074-cm^3/s liquid flow rate at pressures ≥ 1585 kPag, as a check on the DMA-CNC measurements. In the new tests, $MnCl_2 \cdot 4H_2O$ solutions were used in place of KNO_3 to facilitate analyzing the MOI samples by INAA. For concurrently collected DMA-CNC data, the volume mean diameter for particles smaller than the lowest DMA channel (10 nm) was assumed to be 8.7 nm. This leads to an uncertainty of ±10% in the volume of the distribution that lies below 10 nm, and a negligible (< 1%) uncertainty in the $VMAD_r$.

Results of the MOI measurements (Table 4) for the Sonicore nozzle at pressures of 2757 and 6893 kPag show that its performance continued to degrade with increasing pressure in this range, as evidenced by smaller amount of mass measured on the backup filter at the higher pressure. Nozzle SSC-2 was identical to SSC-1 except for its smaller (twofold smaller area) liquid orifice diameter, but its performance was far poorer by the same criterion. The better performance of the latter nozzle might be the result of high pressure cavitation which is expected to favor a larger orifice (Kim and Marshall, 1971). Overall, the best results in these tests were obtained for the SSC-1 nozzle at an air pressure of 3447 kPag, for which about 75% of the mass was contained in particles smaller than 42 nm. As indicated in columns A and B, agreement between replicate runs for the SSC-1 nozzle was excellent.

As indicated in Table 4, discrepancies between MOI and corresponding DMA-CNC measurements were significant when atomizing pressures were ≥ 1585 kPag. This was

TABLE 4. Distribution of Manganese Mass as a Function of Particle Size for Air Atomizing Nozzles, Aspirating 3.0 ppm Mn in Absolute Methanol at 0.074 cm^3/s

Stage	D_{50}[a] (nm)	SSC-1 (Round spray) 1585 kPag	SSC-1 (Round spray) 3447 kPag A	SSC-1 (Round spray) 3447 kPag B	SSC-2 1585 kPag	Sonicore 2757 kPag	Sonicore 6893 Kpag
		% /stage					
1	1047	0.45	1.2	1.9	1.8	0.3	1.5
2	540	NDB[b]	1.4	2.5	1.9	1.3	1.5
3	152	1.8	6.8	5.7	14.0	0.7	9.5
4	83	30.0	15.2	12.4	42.3	19.7	21.9
5	42	1.7	1.2	1.4	0.95	1.4	1.3
6	< 42	65.2	74.4	75.7	38.8	69.6	64.3
DMA-CNC	< 42	47	49	50	—	69	54

[a]Diameter of unit density particle collected with 50% efficiency.
[b]Not determined above blank.

especially true for aerosol made with nozzle SSC-1, for which mass (or volume) in particles smaller than 42 nm was 28% less for DMA-CNC measurements than for the MOI measurement at 1585 kPag and 34% less at 3477 kPag. Also, the MOI data show a more pronounced peak on stage 4, i.e., aerodynamic diameter of 83 nm, than is evident in the DMA-CNC data. In Table 3, estimates of the mass median diameter ($MMAD_r$) of residue particles were made form the MOI data using estimates of the geometric standard deviation (σ_g) for the aerosol as determined from cumulative plots of simultaneously collected DMA-CNC spectra. For example, at an atomizing air pressure of 1585 kPag, the σ_g was 1.7 ± 0.3. The uncertainty is half the difference between the value determined from the 84th and 16th percentiles. As both instruments size particles aerodynamically, the $VMAD_r$ and $MMAD_r$, respectively, determined should be identical. They are not, however, because the MOI consistently indicates that more mass resides in particles smaller than 42 nm.

For data collected when atomizing pressures were ≥ 1585 kPag, we place more confidence in the MOI estimates, as measurements with the DMA-CNC were subject to large diffusional losses, which may have been exacerbated by substantial particle charge induced in the atomization process. Effects of particle charge were not considered in correcting for losses in the probe used to aspirate sample to the DMA-CNC. (Excess particle charge in the DMA-CNC is neutralized with an internally mounted ^{85}Kr source.) Moreover, the efficiency of the CNC depends on flow rate and trigger level (Su et al., 1990). Median residue sizes of Mn-containing particles calculated on the basis of MOI data were 30 ± 3 for the SSC-1 nozzle and 30 ± 2 for the Sonicore nozzle at pressures of 3447 and 2757 kPag, respectively.

We attempted to determine the size of residue particles made from $MnCl_2 \cdot 4H_2O$ solutions by TEM and made another test with the MOI in which carbon-coated copper grids were attached to the impaction stages and backup filter. However, as indicated in Figure 8, (MOI stage 4 at 50,000-fold magnification), we observed only thin circular patterns made from the deposition of liquid droplets. The X-ray spectra of the droplet residues (Figure 8*b*) showed only Mn and Cl (the two copper peaks are associated with the grid) and thus confirm their identity as the $MnCl_2 \cdot H_2O$ test particles. Even these quite large patterns were difficult to observe clearly and we were unable to

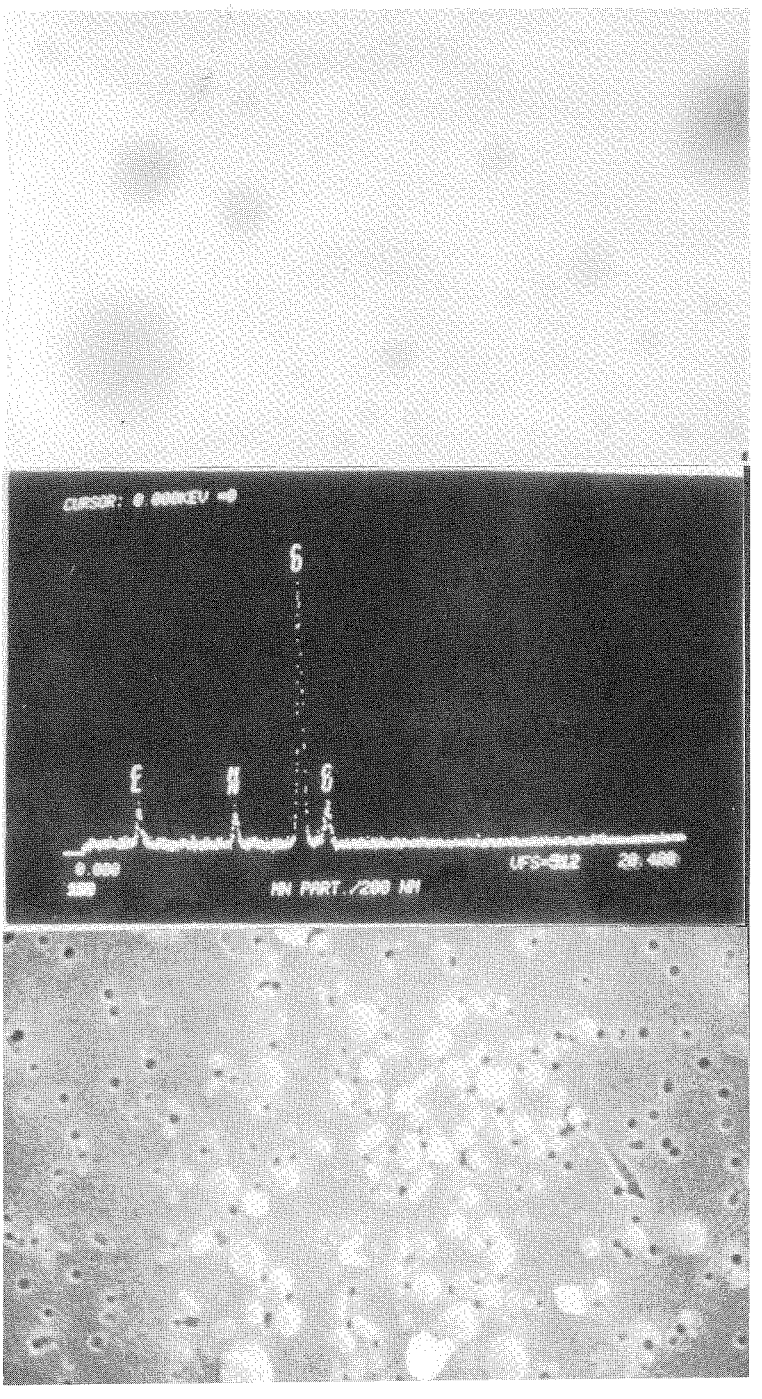

FIGURE 8. (*a*) Transmission electron microscope image and (*b*) single-particle X-ray spectrum show that $MnCl_2$ particles sampled in chamber air were "wet." (*c*) Particles made from KNO_3 were dry.

image residue droplets smaller than 50 nm. As the residue particles collected in laboratory air were clearly droplets, rather than dry solid particles, it is possible that additional size reduction might occur by removing the remaining liquid phase. In our tests, the relative humidity ranged from 20% to 45%. By comparison, Figure 8*c* shows that KNO_3 particles made from methanol solutions were not wet.

Estimation of Droplet Sizes

Droplet median diameters based on aerodynamic size of the residue droplets (also listed in Table 3) were estimated for KNO_3 and Mn-containing particles, assuming a density of 2.1 g/cm^3 for the former. As particles made from the latter were wet, droplet diameters were calculated to reflect the range of possible densities, i.e., 0.78 g/cm^3 (pure methanol) to 2.01 g/cm^3 (pure $MnCl_2 \cdot 4H_2O$). Estimates of median droplet diameters made with the SSC-1 nozzle and KNO_3 solutions range from 6.0 to 3.1 μm, the latter value being achieved at an atomizing pressure of 1585 kPag. Allowing for a 30% uncertainty in the density of residue particles made from KNO_3 solutions, the uncertainty in droplet diameter would be about 9%. Calculated median droplet diameters made with the $MnCl_2 \cdot 4H_2O$ solutions at 1585 kPag with this nozzle were 2.2 $\pm$ 0.3 μm for DMA-CNC measurements, which, may be significantly smaller than those made with KNO_3 solutions at the same pressure. The droplet median diameter calculated from the MOI measurement at this pressure was 1.7 $\pm$ 0.4 μm, a difference of about 20%. The uncertainty in this value and other MOI-derived values listed reflect the range in estimates of the geometric standard deviation of the aerosol obtained from the DMA-CNC data. The MOI-derived results suggest that aerosol with droplet median diameters as small as 1.5 $\pm$ 0.3 were made with both the SSC-1 and Sonicore nozzles at pressures of 3447 and 2757 kPag, respectively.

CONCLUSIONS

We have made residue particles of KNO_3, a salt nondeliquescent salt at relative humidities used here, with MMADs as small as 25 and 35 nm with two commercial air atomizing nozzles at a modest atomizing air pressure of 1585 kPag and liquid flow rate of 0.074 cm^3/s in laboratory air. The MMADs of residue particles made from $MnCl_2 \cdot 4H_2O$ solutions sprayed in chamber air were as small as 30 nm at atomizing air pressures of 3447 and 2757 kPag with two different nozzles. Median droplet diameters calculated for Mn particles were < 2 μm for a Spraying Systems nozzle at a liquid flow rate of 0.074 cm^3/s and atomizing pressures $\geq$ 1585 kPag. This represents an approximately 10-fold increase in liquid flow rate over laboratory Collison atomizers which are capable of producing similarly-sized droplets at liquid flow rates of only 0.0075 cm^3/s.

We thank Zhong Yu Wu for assisting in data reduction. This work was funded by the Electric Power Research Institute, under contract no. RP-2199-03.

REFERENCES

Agarwal, J. K., and Sem, G. J. (1980). *J. Aerosol Sci.* 11:343-357.

Anderson, J. D. Jr. (1982). *Modern Compressible Flow.* McGraw-Hill, New York.

Bartz, H., Fissan, H., Helsper, C., Kousaka, Y., Okuyama, K., Fukushima, N., Keady, P. B., Kerrigan, S., Fruin, S. A., McMurry, P. H., Pui, D. Y. H., and Stolzenburg, M. R. (1985). *J. Aerosol Sci.* 16:443-456.

BGI, Inc. (1990). *Aerosol Instrumentation.* BGI, Inc., Waltham, MA.

Gibb, F. R., Utell, M. J., and Morrow, P. E. (1990). *Aerosol Sci. Technol.* 12:376-385.

Kim, K. Y. and Marshall, W. R. Jr. (1971). *AIChE J.* 17:575-584.

Kuhlmey, G. A., Liu, B. Y. U., and Marple, V. A. (1981). *Am. Ind. Hyg. Assoc. J.* 42:790-795.

Marple, V. A., Liu, B. Y. U., and Kuhlmey, G. A. (1981). *J. Aerosol Sci.* 12:333–337.

Marple, V. A., and Rubow, K. L. (1984). Final Report, Particle Technology Laboratory Publication No. 522. Mechanical Engineering Department, University of Minnesota, Minneapolis.

Mercer, T. T. (1973). In *Aerosol Technology in Hazard Evaluation*. Academic Press, New York, pp. 343–344.

Ondov, J. M., and Kelly, W. R. In *Emissions from Combustion Processes: Origin, Measurement, Control* (R. E. Clement and R. O. Kagel, eds). Lewis Publishers, Chelsea, MI, in press.

Parker, G. J. (1968). *Atmos. Environ.* 2:477–490.

Reineking, A., and Porstendorfer, J. (1986). *Aerosol Sci. Technol.* 5:483–486.

Su, Y. F., Cheng, Y. S., Newton, G. J., and Yeh, H. C. (1990). *Aerosol Sci. Technol.* 12:1050–1054.

Received August 28, 1990; accepted March 18, 1991.